

## CHEMICAL STRUCTURE AND PYROLYSIS RESPONSE OF $\beta$ -O-4 LIGNIN MODEL POLYMER

Jiang-Yan Liu,<sup>a,b</sup> Shu-Bin Wu,<sup>a,\*</sup> and Rui Lou<sup>a</sup>

Hydroxyphenyl (H-type) and guaiacyl (G-type) lignin model polymers composed of the  $\beta$ -O-4 structure without  $\gamma$ -hydroxymethyl groups were synthesized. The chemical structures of the H- and G-type lignin models were characterized by <sup>1</sup>H- and <sup>13</sup>C-NMR, as well as MALDI-TOF/MS. The pyrolysis response was analyzed by means of TG-DTG, Py-GC/MS, and a tube furnace technique. <sup>1</sup>H-, <sup>13</sup>C-NMR, and MALDI-TOF/MS showed that the lignin models were linear polymers. The polymers included the  $\beta$ -O-4 linkage, as in natural lignin. Pyrolytic products from H-type lignin model only possessed *p*-hydroxyphenyl structure without methoxyl groups, and the pyrolytic products from G-type lignin model only possessed guaiacyl structure with methoxyl groups. Pyrolysis products from H- and G- type lignin models were classified into char, gas, and liquid (bio-oil), and the gaseous products of two model compounds mainly consisted of H<sub>2</sub>, CO, CH<sub>4</sub>, CO<sub>2</sub>, and C<sub>2</sub>H<sub>4</sub>.

*Keywords:* Lignin; Hydroxyphenyl; Guaiacyl;  $\beta$ -O-4; Pyrolysis; GC/MS

*Contact information:* a: State Key Lab of Pulp & Paper Engineering, South China University of Technology, Guangzhou, 510640, China; b: College of Chemistry and Environmental Engineering, Hubei Normal University, Huangshi, 435002, China. \* Corresponding author: shubinwu@scut.edu.cn

### INTRODUCTION

Biomass as a renewable energy sources is an important part in developing new energy systems and has been paid more attention recently (Caputo et al. 2005). For example, the technology of biomass thermochemical converting has received intense focus (Hoogwijk et al. 2003). Biomass is mainly composed of cellulose, hemicelluloses and lignin. Recently, biochemical conversion of cellulose and hemicelluloses has made some progress (Ishimaru et al. 2007). Besides cellulose, lignin is the most abundant component in biomass. Lignin is also a very important renewable resource. Degradation of lignin is different from degradation of cellulose due to its complicated structure. Though lignin pyrolysis dynamics and reaction mechanism has been studied by many people (Nakamura et al. 2008; Liu et al. 2008; Drage et al. 2002), knowledge of lignin pyrolysis is very limited except for the studies of the weight-loss behavior and characterization of the low MW products. Thus, the study of the thermal decomposition and pyrolysis behaviors about lignin, and in particular lignin model oligomers that are more similar to original lignin on the structure, is very important to understand biomass thermo-chemistry transformation mechanisms.

Lignin's most basic structural units are of phenyl propane type. These include the three basic types hydroxyl phenyl (H-type), guaiacyl (G-type), and syringyl (S-type). The lignin macromolecules are formed through different internal connections. Among these

linkages, the  $\beta$ -O-4 linkage is the most important and most abundant substructure in lignin, probably accounting for 50% of all linkages. Such a complicated structure causes very great difficulties to study the pyrolysis mechanism.

Model compound research approach offers a possibility to research complicated systems such as lignin. Recently, various lignin model compounds were synthesized (Kawai et al. 1999; Kishimoto et al. 2008) and used for studying themolysis or pyrolysis (Omori 1981; Faix et al. 1988), but there has been little research about the pyrolysis behavior of lignin model oligomer (Enoki et al. 1981; Kawamoto et al. 2007). This work synthesized two types of lignin model oligomer compounds (H-type and G-type) that include the native  $\beta$ -O-4 linkage. The tube furnace pyrolysis device was used to pyrolyze a lignin model oligomer under different temperatures. We have investigated the relationship between products and temperatures for the lignin model oligomer in the pyrolysis process.

## EXPERIMENTAL

### Sample Preparation

The monomers 4-hydroxy-acetophenone and acetovanillone (98%, refined by ether/n-hexane) were obtained from the EHSY company.

Referring to the methods of Kishimoto et al. (2008), the synthesis process of lignin model polymer was divided into three steps: First, the acetophenone derivative (1) (acetovanillone and 4-hydroxy-acetophenone) was dissolved in  $\text{CHCl}_3$ -EtOAc (1:1, v/v), adding  $\text{CuBr}_2$  and a small amount of ethanol to the mixture, then refluxed under nitrogen for 4h to prepare the bromides (2). Second, adding  $\text{K}_2\text{CO}_3$  as the catalyst, the bromides were dissolved in DMF, stirred at  $50^\circ\text{C}$  for 4h under nitrogen, and polymerized to the given polymer (3). Third, the given polymer (3) was reduced with DMSO and  $\text{NaBH}_4$  to obtain the H- and G-type lignin model polymers containing only the  $\beta$ -O-4 linkage (4). Synthetic routes are shown in Fig. 1.

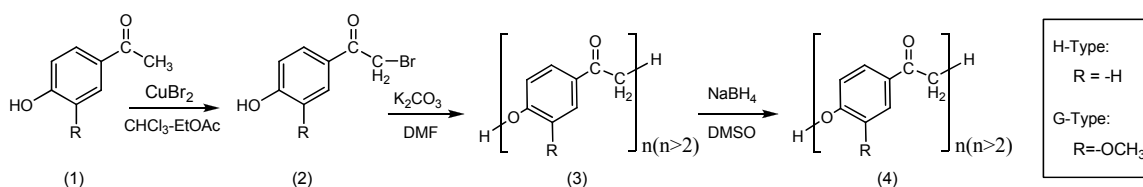


Fig. 1. Synthetic route for H- and G-type lignin models

### Analytical Methods

#### Nuclear magnetic resonance (NMR)

The samples were dissolved in the solvent ( $\text{CDCl}_3$ ), then they were scanned on a  $^1\text{H}$  nuclear magnetic resonance spectrometer (NMR, Bruker Company, Germany) at 400 MHz.

The samples were dissolved in  $\text{DMSO-d}_6$  (99.8% D), then analyses were carried out with a  $^{13}\text{C}$  NMR at 100.6MHz to collect  $^{13}\text{C}$  spectra. Tetramethylsilane (TMS) was added to serve as the internal standard.

### *MALDI-TOF-MS*

MALDI-TOF-MS (Matrix-Assisted Laser Desorption Ionization - Time of Flight Mass Spectrum) spectra were acquired on a Bruker Autoflex III smartbean MALDI-TOF-MS instrument (Bruker, Bremen, Germany). The matrix compound was gentisic acid DHB (2,5-dihydroxy benzoic acid, Bruker Daltonic Leipzig, Germany) dissolved in tetrahydrofuran. The MS measurements were done in the linear mode. For positive ion spectra 200 laser shots were applied.

### *Gel Permeation Chromatograph (GPC)*

The samples were dissolved in tetrahydrofuran. A series of polystyrene samples served as standards. GPC was carried out on a GPCV2000 instrument (Waters 515-410, Alliance Company) with a Waters Styragel HT3 pillar at 35°C. The flow velocity of samples was 0.5ml·min<sup>-1</sup>.

### *Thermogravimetric analysis (TGA)*

Samples were evaluated with a Thermogravimetric Analyzer (TAQ500, NETZSCH Germany) under nitrogen flow of 40 mL/min at a fixed heating rate of 10 °C/min. The temperature range was from room temperature to 800 °C. The data of weight loss rate was collected with TA Instruments Universal Analysis Software.

### *Py-GC/MS method*

The pyrolysis (Chemical Data Systems 5150 (CDS5150), USA) unit is an analytical scale pyrolysis unit which consists of an inductive heated coil to heat samples. The sample was placed in the centre of the inductive coil with an isothermal setting of 600°C and a heating rate of 10°C /ms, pyrolysis hold for 10s, and helium as the carrier gas.

A gas chromatograph (QP2010, Japan) with a split ratio of 70:1 was used for compound separation. The injector and detector temperatures were both at 250 °C. The carrier velocity was 40 cm/s, and the temperature program began with 50 °C for 5 min, then with a heating rate of 10 °C/min to a temperature of 280 °C; the interface temperature was 250°C. The semipolar column DB 1701 (30m by 0.25 mm with 0.25 µm) which shows an electron impact mass spectrum were obtained using a QP2010 Plus at an EI ionization energy of 70 eV. The mass range from m/z 45 amu to 600 amu was scanned with a speed of 1.0 s/decade. Data processing was performed using Perkin Elmer NIST Spec Version 5.

### *Tube furnace pyrolysis methods*

Pyrolysis was carried out in a programmable tubular reactor (see Fig. 2). Briefly, the reactor consisted of a cylindrical quartz glass tube heated by a stainless steel block furnace. A chromel/alumel thermocouple was placed inside the furnace, embedded in the tube, to measure the temperature. A porcelain boat containing samples spread as a thin layer was placed in the middle from the downstream end of the tube, and nitrogen as the carrier gas was used in pyrolysis runs. The furnace initially was heated over an empty portion of the tube and was equilibrated at the desired temperature of 500, 600, 700, 800, and 900°C, respectively. After the desired temperature was reached, the sample was

rapidly moved into the furnace to initiate pyrolysis. The runs were made at atmospheric pressure and at the desired temperatures ranging from 400 to 900°C under approximately isothermal conditions. Reaction time of lignin model pyrolysis was kept the same (5 min) at each temperature, and the heating rate was assumed to be constant. The gaseous products released through an ice-water condenser then were collected. The condensed liquid products that were absorbed in the condenser were defined as tar. At the end of the run, the solid products (char) were allowed to cool to ambient temperature before being recovered. It was stored over dry silica gel under vacuum until analyzed.

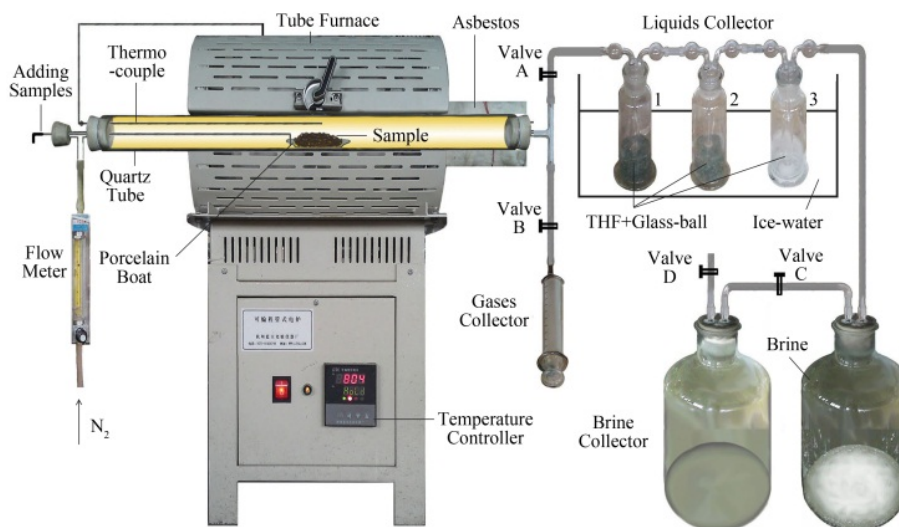


**Fig. 2.** Programmable tube furnace pyrolysis reactor

### *Products analysis*

Gas released from samples during pyrolysis was analyzed on a gas chromatograph (SHIMADZU GC-20B Japan) with a thermal conductivity detector (TCD). The C-RID area method was used to mensurate the proportion of gas component, and argon was used as carried gas at a flow rate of 77.5 mL/min.

Bio-oil was diluted to the right concentration to detect on a GC/MS analyzer (HP-5MS Agilent 2170, USA) with a thin film (30m×0.25mm, 0.5µm film thickness) DB-5 MS capillary column. Carrier gas was the highest purity helium with a flow rate of 0.8 mL/min. The temperature program was 150°C for 3min, heated up to 280°C at 8°C/min, and kept for 20 min. Electron energy with EI ionization mode was 70eV and the interface temperature was held at 250°C. Data processing was carried out with Perkin Elmer NIST08 software.

## RESULTS AND DISCUSSION

### **Molecular Weight of Oligomers**

Molecular weight distributions of lignin model polymers were determined by gel permeation chromatography (GPC) in tetrahydrofuran at 40 °C. The results showed that

the number-averaged molecular weight and polydispersity (DP<sub>n</sub>) of H-type and G-type lignin models were 8285, 4832, and 1.26, 1.21, respectively. The molecular weights of these polymers were comparable to those of technical lignin (see Fig. 3).

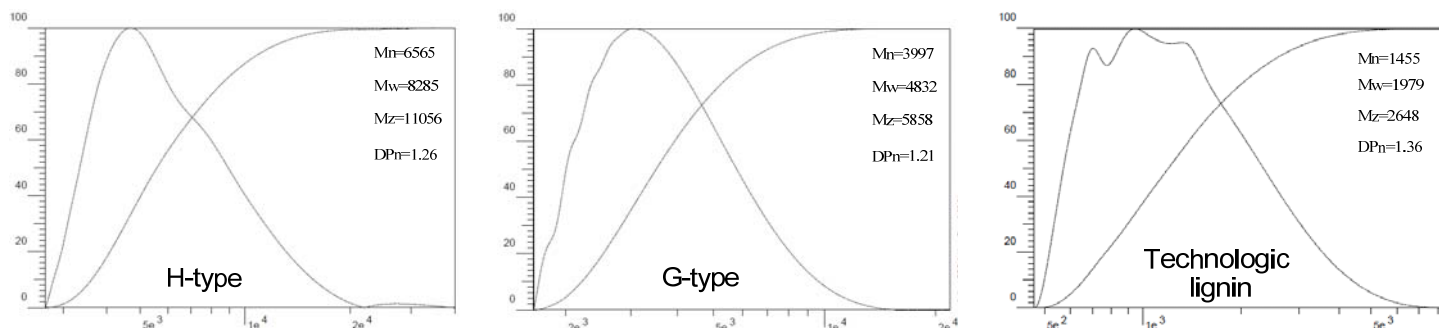


**Fig. 3.** GPC of H- and G-type lignin models

The concentration of the starting monomer is one of the most important factors affecting the degree of polymerization. Lowering of the monomer concentration resulted in an increase in DP<sub>n</sub>. This is probably because the amount of solubilized polymer increased in the diluted solution during polymerization. The effects of reaction temperature were also investigated, DP<sub>n</sub> increased as the reaction temperature rose in the range 50 °C to 100 °C. The increase of reaction temperatures magnified the solubility of polymer and avoided undesirable precipitation during polymerization. Some side reactions may have been involved in this case.

### <sup>1</sup>H- and <sup>13</sup>C-NMR Analysis

The solubility of the lignin related polymers in organic liquids is one of their most important properties. Ordinary solvents could not dissolve carbonyl polymers (compound 3 in Fig.1) at room temperature. Hence, solution NMR spectroscopic analysis of the polymers could not be conducted. However, lignin polymers (compound 4 in Fig.1) could be dissolved in several solvents, such as dioxane, ether, DMF, THF, and DMSO.

The NMR spectra of H- and G-type lignin models are presented in Fig.4, and the spectral analysis is listed in Table 1.

From Table 1, In <sup>1</sup>H-NMR, δ1.26-1.27 is signal of end CH<sub>3</sub>, δ2.48-2.53 is signal of α-position OH, δ3.56 is signal of OCH<sub>3</sub>, δ3.93-3.99 is signal of β-H, δ 4.83-5.47 is signal of α-H, δ6.66-7.32 are signal of C<sub>2</sub>-C<sub>6</sub> in aryl ring. The integral area of β-H is about double the integral area of α-H, which is in agreement with their formula structure. In <sup>13</sup>C-NMR, The distinct sharp signals of all carbons indicate that the polymer has a highly regulated structure, and the polymer actually exists as a mixture of many isomers that have a chiral center at the α-position. Respectively, For H-type and G-type model C<sub>β</sub> signals appear at δ73.61, and δ74.71, C<sub>α</sub> signals appear at δ71.17 and δ71.16, which is similar with some dimer (Ralph et al. 2004). Without C<sub>γ</sub> signal in <sup>13</sup>C-NMR and without C<sub>γ</sub>-OH signal in <sup>1</sup>H-NMR. It may judge the structure without C<sub>γ</sub> and γ-OH only included β-O-4 linkages in model compounds.

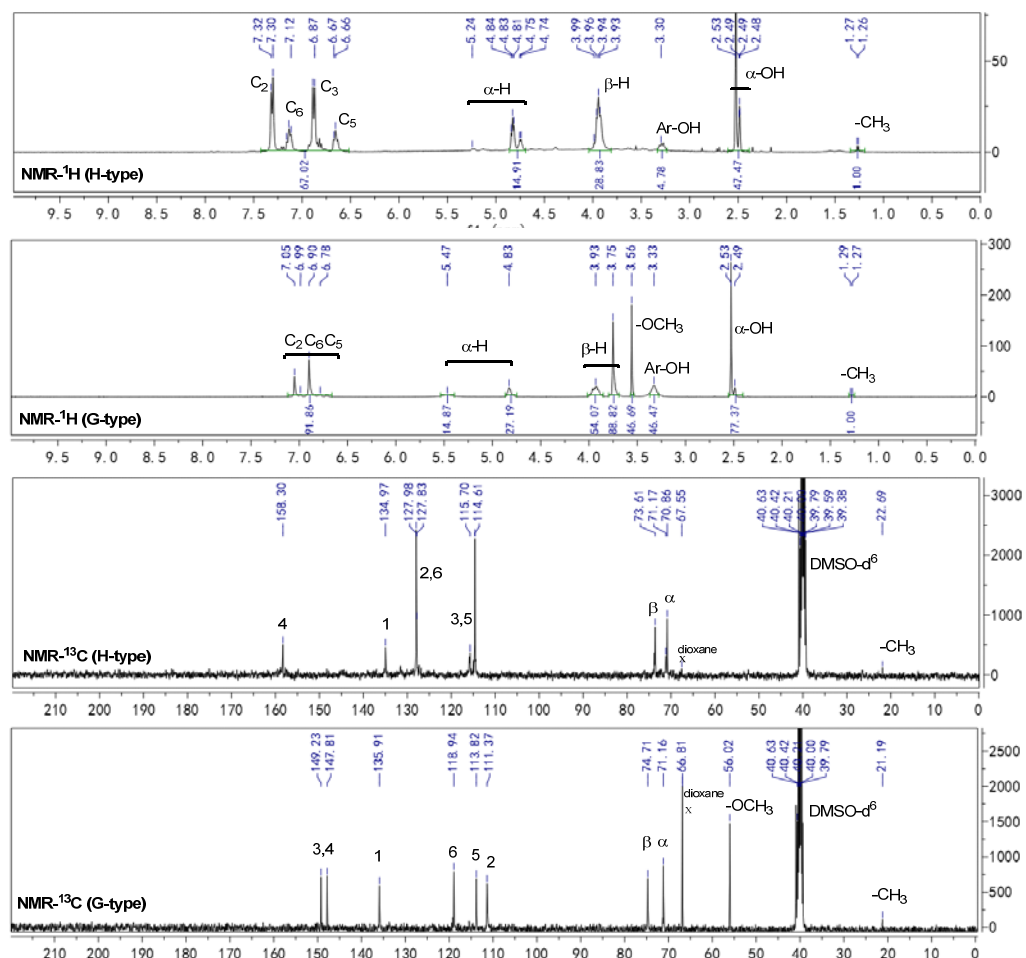


Fig. 4.  $^1\text{H}$  and  $^{13}\text{C}$  NMR of H- and G-type lignin model

Table 1. Chemical Shift of NMR of H-type and G-type Lignin Models

	H-type		G-type	
$^1\text{H}$ NMR	7.32~7.14	$\text{C}_2\text{-H}, \text{C}_6\text{-H}$	7.05~6.99	$\text{C}_2\text{-H}, \text{C}_6\text{-H}$
	6.87~6.63	$\text{C}_3\text{-H}, \text{C}_5\text{-H}$	6.90~6.70	$\text{C}_5\text{-H}$
	4.83~4.74	$\text{C}_\alpha\text{-H}$	5.47~4.82	$\text{C}_\alpha\text{-H}$
	3.99~3.27	$\text{C}_\beta\text{-H}$	3.93~3.75	$\text{C}_\beta\text{-H}$
	2.53~2.48	$\text{C}_\alpha\text{-OH}$	2.53~2.49	$\text{C}_\alpha\text{-OH}$
	1.27~1.26	$\text{-CH}_3$	1.29~1.27	$\text{-CH}_3$
			3.56~3.33	$\text{-OCH}_3$
$^{13}\text{C}$ NMR	158.30	$\text{C}_4$	149.23~147.81	$\text{C}_4, \text{C}_3$
	134.97	$\text{C}_1$	135.91	$\text{C}_1$
	127.98~127.83	$\text{C}_2, \text{C}_6$	118.93	$\text{C}_6$
	115.70~114.61	$\text{C}_3, \text{C}_5$	113.81~111.37	$\text{C}_5, \text{C}_2$
	73.61	$\text{C}_\beta$	74.71	$\text{C}_\beta$
	71.17	$\text{C}_\alpha$	71.16	$\text{C}_\alpha$
	22.69	$\text{CH}_3$	21.19	$\text{CH}_3$
			56.02	$\text{OCH}_3$

### MALDI-TOF-MS Analysis

MALDI-TOF-MS (Matrix-Assisted Laser Desorption Ionization-Time of Flight Tandem Mass Spectrometer) is a relatively new and accurate mass spectroscopic technique that has been employed in the absolute molar mass analysis of synthetic polymers. The main features of the MALDI-TOF-MS technique are high sensitivity, wide mass range, and no fragmentation of the molecules. The interpretation of results is facilitated by the fact that single charged ions are almost exclusively generated. Therefore, the mass to charge ratio of the ions formed by MALDI corresponds directly to the absolute molar mass of the analyte.

The H-type lignin model polymer was analyzed by MALDI-TOF-MS (See Fig.5). The results showed that the polymer has a linear structure and the repeat unit formula weight of the polymer agreed with the expected structure. Molecular masses were found to be given by  $136.16n + 2$ , where  $n$  is the degree of polymerization. This indicates that the polymers have regular structures and that reduction of carbonyl groups at  $\alpha$ -position was successfully conducted under the conditions used. Bromine at the end group was also removed by the reduction with  $\text{NaBH}_4$ .

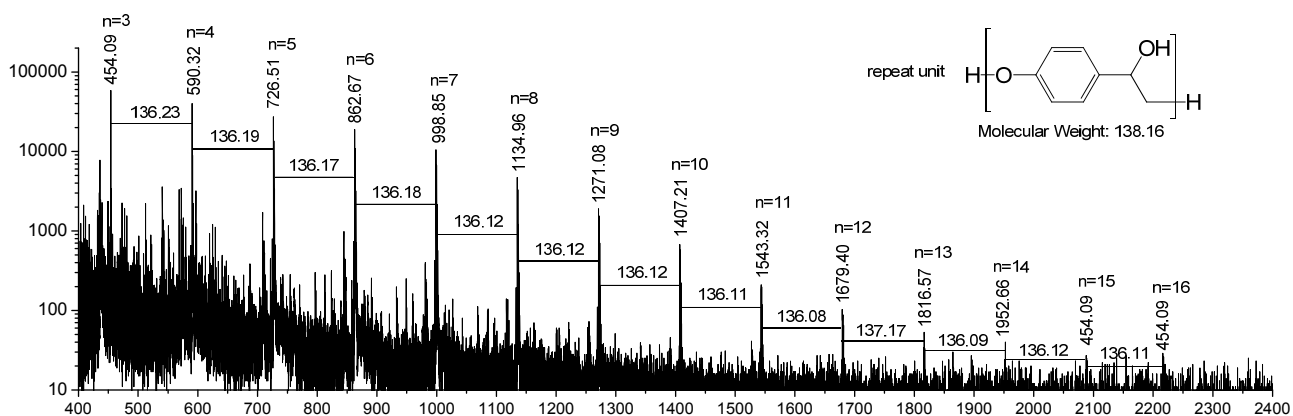


Fig. 5. MALDI-TOF/MS of H-type lignin model polymer

### Pyrolysis-GC/MS analysis

Total ion current (TIC) data from Py-GC/MS of H- and G-type lignin models at  $600^\circ\text{C}$  are shown in Fig. 6, and pyrolysis products from H- and G-type lignin model compounds with Py-GC/MS are listed as Table 2. The pyrolysis products were phenolic compounds, of which the pyrolytic products from H-type lignin model only possessed *p*-hydroxyphenyl structure without any methoxyl group, and the pyrolytic products from G-type lignin model only possessed guaiacyl structure with methoxyl groups. The relative areas of peaks showed that the products mainly were 2,3-dihydro-benzofuran (24.10%), phenol (17.52%), 4-ethyl-phenol(6.17%), 4-methyl-phenol (4.78%) and benzofuran (2.42%) for H-type, and 4-ethenyl-2-methoxy-phenol (38.3%), 4-methoxy-phenol (9.03%), 2,3-dihydro-benzofuran (3.57%), 4-hydroxy-3-methoxy-acetophenone (3.85%), 4-ethenyl-1,2-dimethoxy-benzene (2.81%), vanillin (2.38%) for G-type.

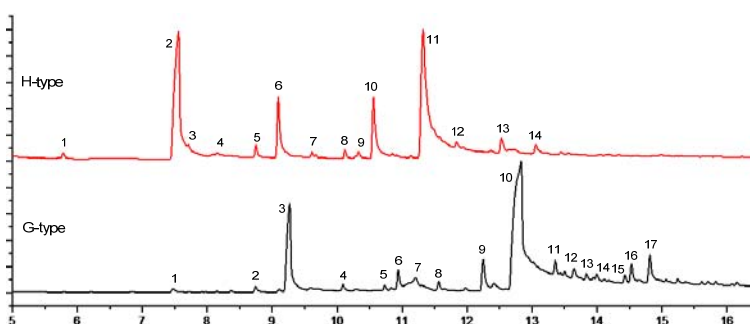


Fig. 6. TIC of Py-GC/MS of H- and G-type lignin models

Table 2. Pyrolysis Products from H- and G-type Lignin Model with Py-GC/MS

No.	R.Time/min	Name	Area%	Formular	MW	Qual
Compounds derived from H-type lignin model						
1	5.78	Styrene	0.34	C <sub>8</sub> H <sub>8</sub>	104	97
2	7.56	Phenol	17.52	C <sub>6</sub> H <sub>6</sub> O	94	99
3	7.71	Benzofuran	2.42	C <sub>8</sub> H <sub>6</sub> O	118	97
4	8.08	Phenol	0.37	C <sub>6</sub> H <sub>6</sub> O	94	99
5	8.75	2-methyl-Phenol	0.72	C <sub>7</sub> H <sub>8</sub> O	108	97
6	9.09	4-methyl-Phenol	4.78	C <sub>7</sub> H <sub>8</sub> O	108	99
7	9.61	2-methyl-Benzofuran	0.25	C <sub>9</sub> H <sub>8</sub> O	132	92
8	10.12	2-ethyl-Phenol	0.52	C <sub>8</sub> H <sub>10</sub> O	122	97
9	10.33	1,2-Benzenedimethanol	0.56	C <sub>8</sub> H <sub>10</sub> O <sub>2</sub>	138	85
10	10.56	4-ethyl-Phenol	6.17	C <sub>8</sub> H <sub>10</sub> O	122	98
11	11.32	2,3-dihydro-Benzofuran	24.10	C <sub>8</sub> H <sub>8</sub> O	120	91
12	11.84	4-(2-propenyl)-Phenol	1.22	C <sub>9</sub> H <sub>10</sub> O	134	90
13	12.53	4-Isopropenylphenol	1.18	C <sub>9</sub> H <sub>10</sub> O	134	91
14	13.06	p-Hydroxyallylbenzene	0.83	C <sub>9</sub> H <sub>10</sub> O	134	90
Compounds derived from G-type lignin model						
1	7.47	Phenol	0.29	C <sub>6</sub> H <sub>6</sub> O	94	98
2	8.76	2-methyl-Phenol	0.39	C <sub>7</sub> H <sub>8</sub> O	108	97
3	9.27	4-methoxy-Phenol	9.03	C <sub>7</sub> H <sub>8</sub> O <sub>2</sub>	124	98
4	10.28	3,4-dimethyl-Phenol	0.18	C <sub>8</sub> H <sub>10</sub> O	122	94
5	10.55	4-ethyl-Phenol	0.13	C <sub>8</sub> H <sub>10</sub> O	122	96
6	10.83	2-methoxy-5-methyl-Phenol	1.98	C <sub>8</sub> H <sub>10</sub> O <sub>2</sub>	138	95
7	11.21	2,3-dihydro-Benzofuran	3.57	C <sub>8</sub> H <sub>8</sub> O	120	91
8	11.56	1,2-dimethoxy-3-methyl-Benzene	0.52	C <sub>9</sub> H <sub>12</sub> O <sub>2</sub>	152	93
9	12.25	4-ethyl-2-methoxy-Phenol	3.53	C <sub>9</sub> H <sub>12</sub> O <sub>2</sub>	152	94
10	12.83	4-ethenyl-2-methoxy-Phenol	38.30	C <sub>9</sub> H <sub>10</sub> O <sub>2</sub>	150	89
11	13.36	4-ethenyl-1,2-dimethoxy-Benzene	2.81	C <sub>10</sub> H <sub>12</sub> O <sub>2</sub>	164	92
12	13.65	Vanillin	2.38	C <sub>8</sub> H <sub>8</sub> O <sub>3</sub>	152	96
13	13.84	2-methoxy-4-(2-propenyl)-Phenol	1.65	C <sub>10</sub> H <sub>12</sub> O <sub>2</sub>	164	82
14	14.00	2-methoxy-4-(1-propenyl)-Phenol	1.32	C <sub>10</sub> H <sub>12</sub> O <sub>2</sub>	164	93
15	14.43	2-methoxy-4-propyl-Phenol	1.74	C <sub>10</sub> H <sub>14</sub> O <sub>2</sub>	166	92
16	14.53	2-methoxy-4-propenyl-Phenol	2.01	C <sub>10</sub> H <sub>12</sub> O <sub>2</sub>	164	94
17	14.82	4-hydroxy-3-methoxy-Acetophenone	3.85	C <sub>9</sub> H <sub>10</sub> O <sub>3</sub>	166	97



### Tube Furnace Pyrolysis

Pyrolysis products from H- and G- type lignin models were classified into char, gas, and liquid (bio-oil), and the yields of products are listed in Table 3. As shown in the table, the pyrolysis products were different from technologic lignin (Wu et al. 2008), and they did not contain five-membered rings from cellulose pyrolysis.

With increasing pyrolysis temperature, as a whole, the char yield decreased and the yield of gas increased, while the yield of liquid accounted for a huge proportion, based on mass fraction. Yields of bio-oil and gas from G-type lignin model pyrolysis exceeded the corresponding H-type. It can be assumed that in this experiment the gasification yield was reduced and liquefaction yield increased notably at 900°C due to the reaction that took place between H<sub>2</sub>, CO, and C<sub>2</sub>H<sub>4</sub> together with other oxidizing components in system, and the reaction then led to the transform of the gases to the liquid.

**Table 3.** Product Yields from H- and G-type Lignin Models vs. Pyrolysis Temperature

Yield/%	H-type lignin model					G-type lignin model				
	500	600	700	800	900	500	600	700	800	900
Gas	4.87	5.41	22.13	21.22	7.42	10.61	17.66	26.96	35.16	7.92
Liquid	45.82	57.61	39.51	45.91	56.96	46.26	50.96	42.13	37.57	64.81
Char	49.31	36.98	38.36	32.87	35.62	43.13	31.38	30.91	27.27	27.27

### Composition analysis of gas

The gaseous products consisted of H<sub>2</sub>, CO, CH<sub>4</sub>, CO<sub>2</sub>, and C<sub>2</sub>H<sub>4</sub> (see Table 4). Among them, the production of CH<sub>4</sub> and CO<sub>2</sub> were hardly subject to being affected by the temperature. The amount of H<sub>2</sub>, CO, and C<sub>2</sub>H<sub>4</sub> increased with increasing temperature and were maximized at 800 °C. However, when the temperature reached 900 °C, gas yield was reduced rapidly. These effects are quite different from what is observed with ordinary biomass pyrolysis or with technical lignin. It may be lead to the hydrogenation and reduction of the methoxyl ArO–CH<sub>3</sub> or phenoxyl Ar–OH cracking at 900 °C, because the compounds with methoxyl and phenoxyl groups disappeared at 900 °C (seen Figs. 7 and 8). The detailed reasons will be further discussed in another paper.

**Table 4.** Composition of Pyrolysis Gas from H- and G-type Lignin Models \*

Temp.°C	H-type lignin model					G-type lignin model				
	500	600	700	800	900	500	600	700	800	900
H <sub>2</sub> (%)	11.21	24.62	36.78	44.03	25.29	16.61	19.48	29.86	33.79	16.18
CH <sub>4</sub> (%)	7.97	3.82	6.21	4.71	2.38	5.42	6.02	5.69	3.86	4.67
CO (%)	4.07	10.28	37.42	45.13	22.81	16.77	30.45	54.92	65.26	6.36
CO <sub>2</sub> (%)	5.84	1.86	2.09	1.52	1.93	2.45	0.91	1.71	1.23	1.06
C <sub>2</sub> H <sub>4</sub> (%)	2.51	8.29	17.83	29.92	8.46	10.24	31.77	25.26	25.98	21.68

\*The content of nitrogen introduced into system was deducted

*Composition analysis of bio-oil*

TIC (total ion current) of bio-oil and the structure of the detected chemicals from H- and G-type lignin models pyrolysis with GC/MS are shown in Figs. 7 and 8.

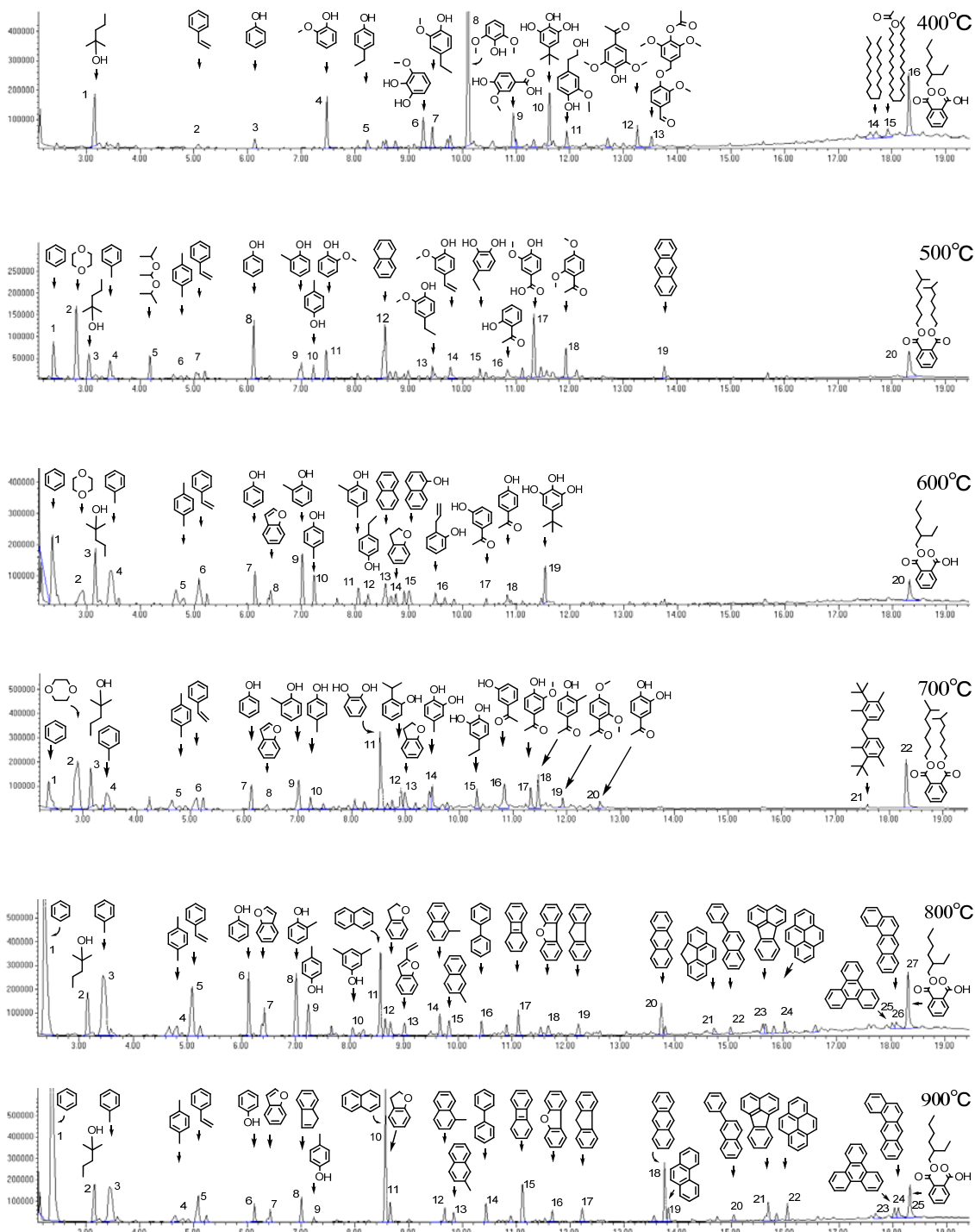


**Fig. 7.** Total ion current of bio-oil from G-type lignin model with GC/MS

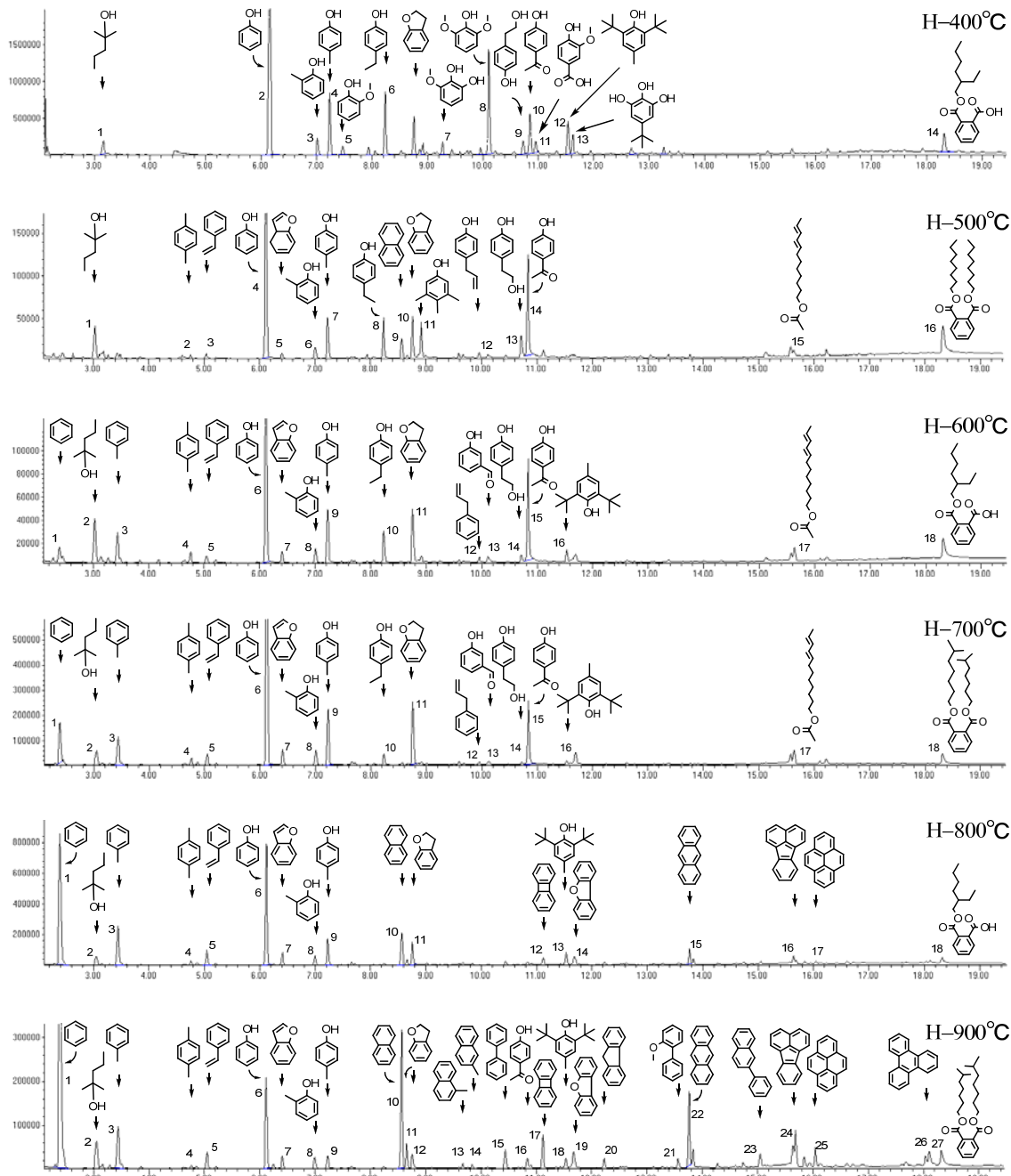


**Fig. 8.** Total ion current of bio-oil from H-type lignin model with GC/MS

From Fig. 7, it is apparent that the pyrolysis temperature had an obvious influence on the composition of bio-oil. At 400°C, the compounds of bio-oil were mainly monocyclic oxygenated chemicals. With increasing temperature, the compounds became complicated, and polycyclic aromatic hydrocarbons were generated owing to condensation reactions occurring.

At 400°C, the products were huge amounts of phenolic compounds, i.e. 2-methyl-2-pentanol (7.99%), 2-methoxy-phenol (5.92%), 2, 6-dimethoxy-phenol (32.20%), 1,2-benzenedicarboxylic acid mono(2-ethylhexyl) ester (9.3%), 5-tert-butylpyrogallol (6.53%), and compounds with the aryl-ether linkages (1.19%), etc. At 500°C, the compounds of benzene (6.14%), dioxane (13.27%), toluene (3.60%), naphthalene (11.42%), anthracene (1.64%), and 4-hydroxy-3-methoxybenzoic acid (9.50%) emerged, and the content of phenol increased to 7.99%. The compounds containing ether bonds disappeared, which indicated that the cleavage of ether linkages occurred before 500 °C. At 600 °C the content of benzene and toluene increased to 19.28% and 13.79% respectively, and the content of methyl-phenol increased to 13.8%. At 700 °C, the content of dioxane increased to 15.12%, and the content of phenols began to decrease. At 800°C polycyclic aromatic hydrocarbons brought forth large amounts of naphthalene, biphenyl, biphenylene, pyrene, dibenzofuran, naphthalene, fluorene, phenanthrene, anthracene, fluoranthene, and the cleavage of methoxyl occurred reasonably at 800 °C. At 900 °C the content of benzene, naphthalene, and anthracene increased to 36.89%, 12.08%, and 5.17%, respectively, and polycyclic aromatic hydrocarbons continued to be generated.

From Fig. 8 it is apparent that the composition of bio-oil from H-type lignin model pyrolysis was similar to G-type, but the content of phenol and naphthalene in bio-oil were higher than that from G-type lignin model pyrolysis.

#### *TGA of G-type lignin model*

The thermal decomposition process of G-Type lignin model could be divided into four stages (see Table 5). The results basically agreed with past similar work done on biomass (He et al. 2006) and on lignin (Wang et al. 2008).

**Table 5.** Parameters of G-type lignin model pyrolysis

Temp. /°C	Mass /%	Peak Temp./ °C	Main reason of weight loss
27~120	7.01	99	The emergence of volatile solvent residual in the sample
120~238	13.45	155	The unreacted monomer in the sample pyrolyzing
238~400	34.15	315	Main reaction area of lignin model pyrolysis, the cleavage of aryl ether linkage
400~700	10.40	400	Secondary reaction of pyrolysis products, the cleavage of methoxyl groups
Char yield	34.98%		

#### *Pyrolysis mechanism of G-type lignin model*

The possible pyrolysis pathways (see Fig. 9) of G-type lignin model involved the breaking of bonds, i.e. C<sub>α</sub>-C<sub>β</sub>, C<sub>β</sub>-O, Ar-C<sub>α</sub> and O-4, among which the bonds C<sub>α</sub>-C<sub>β</sub> and C<sub>β</sub>-O are known to be prone to breakage. Such reactions can account for at least some of the pyrolysis products that were detected in Fig. 6. For instance, peaks 3, 4, 5, 7, 11, and 12 at 400°C, peaks 6, 8, 9, 10, 11, 13, 15, and 18 at 500°C, and peaks 5, 6, 7, 9, 10, 11, 12, 17, 18 at 600 °C may be involved in such bond breakage. For the structure with

$\beta$ -O-4, Kawamoto et al. (2007) proposed two ways of pyrolysis reaction, the cleavage of  $C_{\beta}$ -O and the elimination of  $C_{\gamma}$ , and the former reaction leads to an increase of phenolic compounds. Quantum chemistry calculations showed that the  $C_{\beta}$ -O bond (having an energy of 90.9 kcal/mole) was easier to crack than  $C_{\alpha}$ - $C_{\beta}$  (having a bond energy of 103.8 kcal/mole). In comparison, O-4 (with a bond energy of 137.2 kcal/mole) was most stable and next was 1- $\alpha$  (bond energy is 122.5 kcal/mole). Therefore, the polymer tended to form more phenols after pyrolysis.

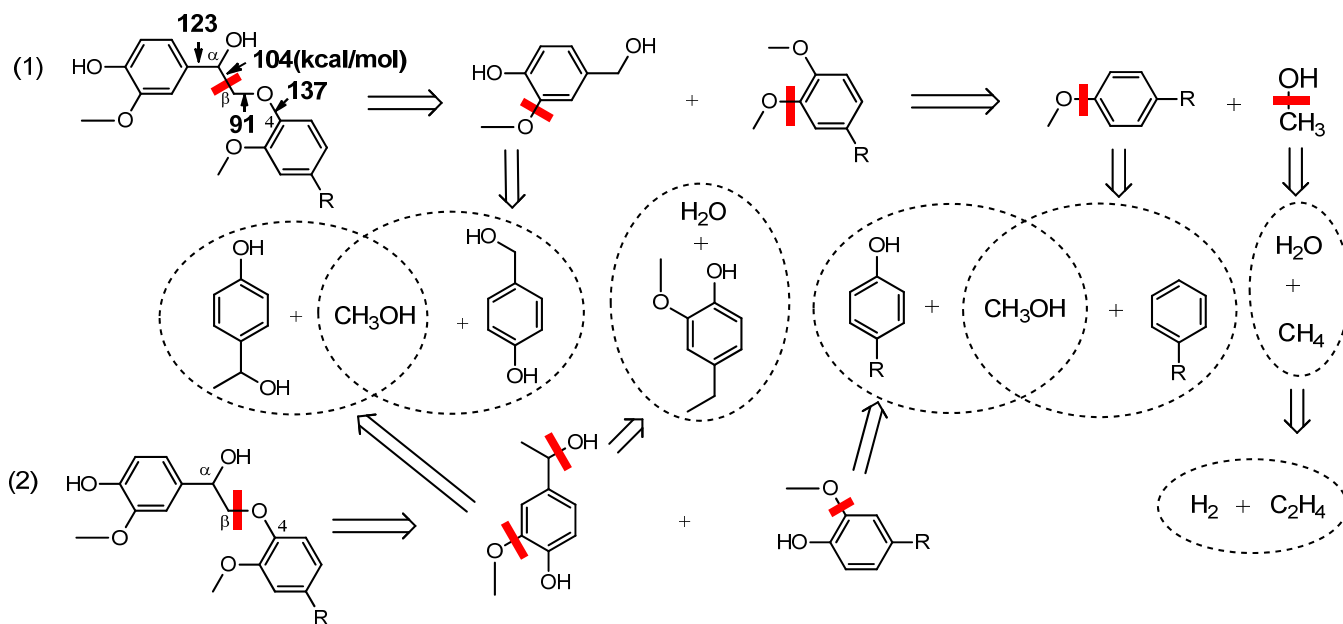


**Fig. 9.** The possible pyrolysis pathways of G-type lignin model

## CONCLUSIONS

The synthetic H- and G-type lignin models compounds were linear polymers. The polymers included the  $\beta$ -O-4 linkage, as in natural lignin. The pyrolysis products of lignin model were simpler than technical lignin or natural lignin, and they did not contain five-membered rings from cellulose pyrolysis.

Py-GC/MS analysis indicated that the pyrolytic products from H-type lignin model possessed only p-hydroxyphenyl structure without any methoxyl groups, and the pyrolytic products from G-type lignin model only possessed guaiacyl structure with methoxyl groups.

Pyrolysis products from H- and G- type lignin models were classified into char, gas, and liquid (bio-oil). With increasing pyrolysis temperature, the char yield decreased and the yield of gas increased. The yield of liquid accounted for a huge proportion of the mass. The compounds of liquid varied and polymerized with an increase of temperature, and oxygenated compounds were reduced, i.e. phenols, methoxyl, and ethers. The

gaseous products consisted of H<sub>2</sub>, CO, CH<sub>4</sub>, CO<sub>2</sub>, and C<sub>2</sub>H<sub>4</sub>. Among them, the production of CH<sub>4</sub> and CO<sub>2</sub> were hardly subject to being affected by the temperature, and the amount of H<sub>2</sub>, CO, and C<sub>2</sub>H<sub>4</sub> were maximized at 800°C, and increased with increasing temperature. But when the temperature reached 900°C, gas yield decreased rapidly, because the chemical activity of small molecules was enhanced at high temperature.

The decomposition of G-type lignin model can be divided into four stages, and the char yield was 34.98% at 700°C. G-type lignin model was pyrolyzed with the cleavage of ether linkages and methoxyl groups, with the re-forming of some phenol molecules. Splitting of C $\alpha$ -C $\beta$  bonds and C $\beta$ -O bonds in  $\beta$ -O-4 structures, as well as the cleavage of ArO-CH<sub>3</sub> bonds in G-type lignin model compounds are the main pyrolysis pathways. These would be useful for understanding of the relationship between the pyrolysis products and structure of lignin models.

## ACKNOWLEDGMENTS

The authors sincerely acknowledge the support by China National Key Basic Research Fund (973 Programme, 2007CB210201) and China National Natural Science Fund(20576043).

## REFERENCES CITED

- Caputo, A. C., Palumbo, M., and Pelagagge, P. M. (2005). "Economics of biomass energy utilization in combustion and gasification plants: Effects of logistic variables," *Biomass and Bioenergy* 28(1), 35-51.
- Drage, T. C., Vane, C. H., and Abbott, G. D. (2002). "The closed system pyrolysis of  $\beta$ -O-4 lignin substructure model compounds," *Organic Geochemistry* 33, 1523-1531.
- Enoki, A., Goldsby, G. P., and Gold, M. H. (1981). "Ether cleavage of the lignin model compound 4-ethoxy-3-methoxyphenylglycerol-guaiacyl ether and derivatives by *Phanerochaete chrysosporium*," *Arch. Microbiol.* 129, 141-145.
- Faix, O., Meiera, D., and Fortmanna, I. (1988). "Pyrolysis-gas chromatography-mass spectrometry of two trimeric lignin model compounds with alkyl-aryl ether structure," *Journal of Analytical and Applied Pyrolysis* 14(2-3), 135-148.
- He, F., Yi, W., and Bai, X. (2006). "Investigation on caloric requirement of biomass pyrolysis using TG - DSC analyzer," *Energy Conversion and Management*. 47, 2461-2469.
- Hoogwijk, M., Faaij, A., and van den Broek, R. (2003). "Exploration of the ranges of the global potential of biomass for energy," *Biomass and Bioenergy* 25(2), 119-133.
- Ishimaru, K., Hata, T., and Bronsveld, P. (2007). "Spectroscopic analysis of carbonization behavior of wood, cellulose and lignin," *J. Mater. Sci.* 42, 122-129.
- Kawai, S., Okita, K., and Sugishita, K. (1999). "Simple method for synthesizing phenolic  $\beta$ -O-4 dilignols," *J. Wood Sci.* 45, 440-443.
- Kawamoto, H., Horigoshi, S., and Saka, S. (2007). "Pyrolysis reactions of various lignin model dimers," *J. Wood Sci.* 53, 168-174.

- Kishimoto, T., Uraki, Y., and Ubukata, M. (2008). "Synthesis of bromoacetophenone derivatives as starting monomers for  $\beta$ -o-4 type artificial lignin polymers," *Journal of Wood Chemistry and Technology* 28, 97-105.
- Liu, Q., Wang, S., Zheng, Y., Luo, Z., and Cen, K. (2008). "Mechanism study of wood lignin pyrolysis by using TG-FTIR analysis," *J. Anal. Appl. Pyrolysis*. 82, 170-177.
- Nakamura, T., Kawamoto, H., and Saka, S. (2008). "Pyrolysis behavior of Japanese cedar wood lignin studied with various model dimers," *J. Anal. Appl. Pyrolysis* 81, 173-182.
- Omori, S., and Dence, C. W. (1981). "The reactions of alkaline hydrogen peroxide with lignin model dimers," *Wood Sci. Technol.* 15, 113-123.
- Ralph, S. A., Ralph, J., and Landucci, L. L. "NMR database of lignin and cell wall model compounds," November 2004. Available at URL <http://ars.usda.gov/Services/docs.htm?docid=10491>
- Wang, G., Li, W., Li, B.-Q., and Chen, H.-K. (2008). "TG study on pyrolysis of biomass and its three components under syngas," *Fuel* 87, 552-558.
- Wu, S.-B., Xiang, B.-L., Liu, J.-Y., Guo, Y.-L., and Sun, R.-C. (2008). "Studies on the pyrolysis characteristics of technical alkali lignin," *Journal of Beijing Forestry University*. 30(5), 143-147.

Article submitted: July 1, 2010; Peer review completed: November 23, 2010; Revised version received and accepted: February 16, 2011; Published: February 18, 2011.